

## Propagation Dynamics of a Particle Phase in a Single-File Pore.

A.M.Lacasta<sup>1</sup>, J.M.Sancho<sup>2</sup>, F.Sagues<sup>3</sup> and G.Oshanin<sup>4</sup>

<sup>1</sup> Departament de Física Aplicada, Universitat Politècnica de Catalunya, E-08028 Barcelona, Spain

<sup>2</sup> Departament d'Estructura i Constituents de la Matèria, Universitat de Barcelona, E-08028 Barcelona, Spain

<sup>3</sup> Departament de Química Física, Universitat de Barcelona, E-08028 Barcelona, Spain

<sup>4</sup> Laboratoire de Physique Théorique des Liquides, Université Paris 6, 75252 Paris, France

### Abstract

We study propagation dynamics of a particle phase in a single-file pore connected to a reservoir of particles (bulk liquid phase). We show that the total mass  $M(t)$  of particles entering the pore up to time  $t$  grows as  $M(t) = 2m(J, \rho_F)\sqrt{D_0 t}$ , where  $D_0$  is the "bare" diffusion coefficient and the prefactor  $m(J, \rho_F)$  is a non-trivial function of the reservoir density  $\rho_F$  and the amplitude  $J$  of attractive particle-particle interactions. Behavior of the dynamic density profiles is also discussed.

### Introduction

Particles transport across microscopic pores is an important step in a vast variety of biological, chemical engineering and industrial processes, including drug release, catalyst preparation and operation, separation technologies, especially biological and biochemical, tertiary oil recovery, drying and chromatography [1, 2, 3].

Man-made or naturally occurring porous materials contain a wide range of pore sizes, from meso- to micro- or even nanoscales, in which case the pore diameter is comparable to the molecular size. Such molecular sized channels, of order of a few Angstroms only, appear, for instance, in biological membranes, and are specific to water and ion transport which participate in hydrostatic or osmotic pressure controlled cellular volume regulation [4]. Carbon nanotubes or zeolites, such as, Mordenite, L, AIPO<sub>4</sub>-5, ZSM-12, may also contain many channels of nearly molecular diameter and can selectively absorb fluids serving as remarkable molecular sieves [5]. For example, AIPO<sub>4</sub>-5 is composed of nonintersecting and approximately cylindrical pores of nominal diameter 7.3 Angstroms.

A salient feature of transport in molecularly sized pores is that there is a dramatic difference between the diffusion of adsorbates whose size is much smaller than the pore diameter, and those whose size is comparable to it. If the diameter of the diffusing guest molecules exceeds the pore radii, but is still less than its diameter, the particles are able to enter the pore but not able to bypass each other such that initial given order is strictly

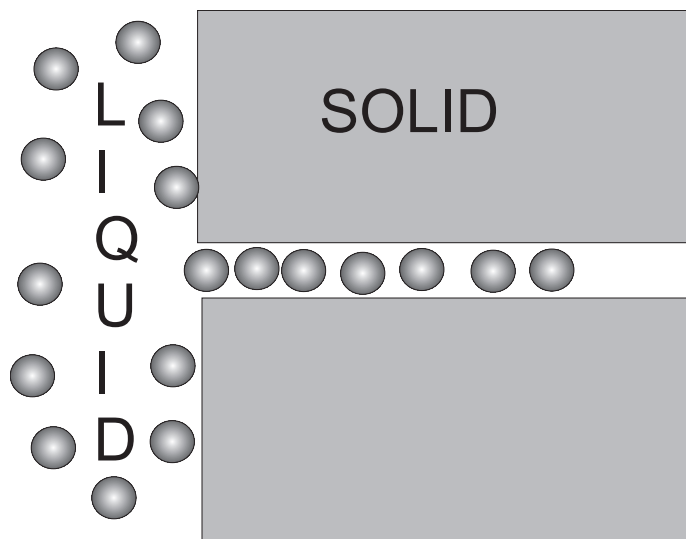


Figure 1: Solid with a single-file pore in contact with a liquid phase.

maintained (see Fig.1). Here, diffusion obeys the so-called "single-file" behavior; the mean-square displacements of tracer molecules do follow  $\overline{X^2(t)} = 2Ft^{1/2}$  [6, 7, 8], where  $F$  is referred to as the "single-file" mobility; evidently, such a behavior is remarkably different from the conventional diffusive law  $\overline{X^2(t)} = 2Dt$ , observed in situations when the guest molecules are able to bypass each other. Single-file diffusion was evidenced by pulsed field gradient NMR measurements with a variety of zeolites and guest species [6, 7]; in particular, the law  $\overline{X^2(t)} = 2Ft^{1/2}$  has been identified experimentally for  $C_2H_6$  [6] and  $CF_4$  [9] in  $AlPO_4-5$ .

Diffusion of absorbed particles in single-file pores has also been the issue of a considerable theoretical interest recently. Several approaches have been proposed, based mostly on the lattice-gas-type models, and such properties as concentration profiles or steady-state particle currents have been evaluated [10, 11, 12]. As well, a great deal of Monte Carlo and Molecular Dynamics simulations has been devoted to the problem [13, 14, 15], providing a deeper understanding of the transport mechanisms in single-file pores. On the other hand, still little is known about non-stationary behavior in single-file systems; in particular, how fast do the particle phase propagates within the single-file pores or how does the total mass (or number) of particles entering the pore up to time  $t$  grows with time?

In the present paper we focus on the challenging question of the particle phase propagation dynamics in the single-file pores. We report here some preliminary results; a detailed account will be published elsewhere [16]. More specifically, we consider a single-file pore in contact with a reservoir of particles (bulk liquid phase), which maintains a fixed particle density at the entrance to the pore. The pore is modelled, in a usual fashion, as a one-

dimensional regular lattice whose sites support, at most, a single occupancy; the particles interaction potential consists of an abrupt, hard-core repulsive part, which insures single-occupancy, and is attractive, with an amplitude  $J \geq 0$ , for the nearest-neighboring particles only. Introducing then a standard, interacting lattice-gas dynamic rules (see e.g. [17]), we derive evolution equation for the local variables describing mean occupation (density) of the lattice sites, which is analysed both analytically and numerically. Within our approach, we define the evolution of the total number  $M(t)$  of particles entering the single-file pore up to time  $t$  and also discuss the dynamics of the density distribution function within the pore. We show that the growth of  $M(t)$  is described by  $M(t) = 2m(J, \rho_F)\sqrt{D_0 t}$ , which can be thought of as the microscopic analog of the Washburn equation, where  $D_0$  denotes the "bare" diffusion coefficient, while the prefactor  $m(J, \rho_F)$  is a non-trivial function of the attractive interactions amplitude  $J$  and the density  $\rho_F$  at the entrance to the pore.

## The model

Following earlier works [10, 11, 12], as well as a conceptually close analysis of an upward creep dynamics of ultrathin liquid films in the capillary rise geometries [18], which appears to be well-adapted to the single-file dynamics, we model the single-file system under study (Fig.1) as a semi-infinite linear chain of equidistantly placed sites  $X$  (with spacing  $\sigma$ ), attached to a reservoir of particles maintained at a constant chemical potential  $\mu$  (see Fig.2). Each pair of sites is separated by a potential barrier of height  $E_B$ , which sets the typical time scale  $\tau_B$ . Note that the spacing  $\sigma$  can be defined, in case of hard solids, as the interwell distance of a periodic potential describing the interactions of the particles with the solid atoms and  $\tau_B$  is related to  $E_B$  and the reciprocal temperature  $\beta = 1/T$  through the Arrhenius formula. For soft solids, in which case the dominant dissipation channel is due to mutual particle-particle interactions,  $\sigma$  can be thought of as the typical distance travelled by particles before successive collisions; here,  $\tau_B$  is just the ballistic travel time.

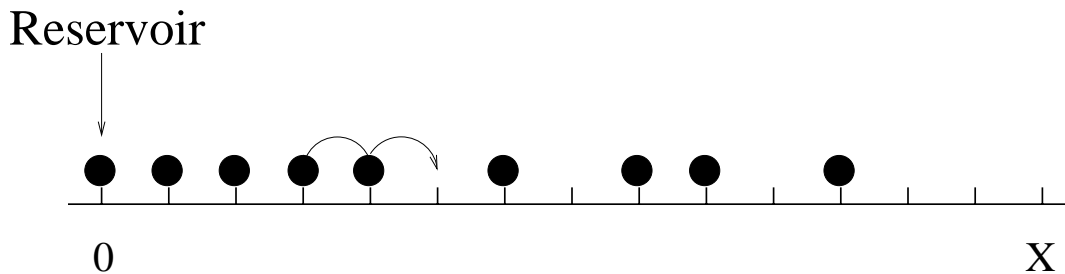


Figure 2: Effective model for transport in a single-file pore.

Further on, we define the particles interaction potential  $U(X)$  as:

$$U(X) = \begin{cases} 0, & X > \sigma, \\ -J, & X = \sigma, \\ +\infty, & X < \sigma, \end{cases} \quad (1)$$

i.e. we suppose that the interaction potential between particles is a hard-core exclusion, which prevents multiple occupancy of any site, and attraction with an amplitude  $J$ , ( $J \geq 0$ ), between the nearest-neighboring particles only. Occupation of the site  $X$  at time moment  $t$  for a given realization of the process will be described then by the Boolean variable  $\eta_t(X)$ , such that

$$\eta_t(X) = \begin{cases} 1, & \text{the site } X \text{ is occupied,} \\ 0, & \text{otherwise.} \end{cases} \quad (2)$$

Consequently, the interaction energy  $U_t(X)$  of the particle occupying at time  $t$  the site  $X$  for a given realization of the dynamical process is

$$U_t(X) = -J(\eta_t(X + \sigma) + \eta_t(X - \sigma)). \quad (3)$$

Lastly, we define the particle dynamics (see [17] for more details). We suppose that at time moment  $t$  any particle occupying site  $X$  waits an exponential time with mean  $\tau_B$  and then selects a jump direction with the probability

$$p(X|X') = Z^{-1} \exp \left[ \frac{\beta}{2} (U_t(X) - U_t(X')) \right], \quad \sum_{X'} p(X|X') = 1, \quad (4)$$

where  $Z$  is the normalization,  $X' (= X \pm \sigma)$  denotes here the target neighboring site and the sum over  $X'$  means the sum over all nearest neighbors of the site  $X$ . As soon as the target site is chosen, the particle attempts to hop onto it; the hop is instantaneously fulfilled if the target site is empty; otherwise, the particle remains at its position. Physically, it means that repulsive interactions are very short-ranged - much shorter than the lattice spacing, and particles "learn" about them only when they attempt to land onto some already occupied site. In turn, attractive interactions are felt within the distance equal to the lattice spacing and hence, influence the choice of the jump direction in order to minimize the total energy of the system.

## Evolution equations

Now, let  $\rho_t(X) = \overline{\eta_t(X)}$ , where the overbar denotes averaging with respect to different realizations of the process. Assuming local equilibrium, we find then that the time evolution of  $\rho_t(X)$  is governed by the following balance equation [16]:

$$\begin{aligned} \tau_B \dot{\rho}_t(X) &= (1 - \rho_t(X)) \left[ \rho_t(X - \sigma) \overline{p(X - \sigma | \sigma)} + \rho_t(X + \sigma) \overline{p(X + \sigma | X)} \right] - \\ &- \rho_t(X) \left[ (1 - \rho_t(X + \sigma)) \overline{p(X | X + \sigma)} + (1 - \rho_t(X - \sigma)) \overline{p(X | X - \sigma)} \right], \end{aligned} \quad (5)$$

where the average transition rate  $\overline{p(X|X')}$  obeys Eq.(4) with  $\eta_t(X)$  replaced by  $\rho_t(X)$ . Equation (5) accounts for the fact that a particle may appear at time moment  $t$  on an *empty* site  $X$  by hopping from the *occupied* sites  $X \pm \sigma$  with corresponding transition probabilities dependent on the interaction energy of the system; and may leave the *occupied* site  $X$  for *unoccupied* sites  $X \pm \sigma$ .

Next, we turn to the so-called diffusion limit, assuming that  $\tau_B$  scales as  $\sigma^2$ ; we thus suppose that  $\sigma \rightarrow 0$ ,  $\tau_B \rightarrow 0$ , but the ratio  $\sigma^2/\tau_B = \text{const} = 2D_0$ , where  $D_0$  is the diffusion coefficient describing motion of an individual, isolated particle. Expanding  $\rho_t(X \pm \sigma)$  and  $\overline{p(X|X \pm \sigma)}$  in the Taylor series up to the second order in powers of the lattice spacing  $\sigma$ , we arrive at the desired dynamical equation of the form

$$\dot{\rho}_t(X) = D_0 \frac{\partial}{\partial X} \left[ \frac{\partial}{\partial X} + \beta \rho_t(X) (1 - \rho_t(X)) \frac{\partial U_t(X)}{\partial X} \right], \quad (6)$$

where  $U_t(X)$  is the interaction energy at point  $X$  defined by Eq.(3).

Now, a few comments on Eq.(6) are in order. Note first that Eq.(6) is a Burgers-type equation with an environment dependent force,

$$\frac{\partial U_t(X)}{\partial X} \approx -2J \frac{\partial \rho_t(X)}{\partial X} - \sigma^2 J \frac{\partial^2 U_t(X)}{\partial X^2}. \quad (7)$$

When only the first term on the rhs of Eq.(7) is taken into account, we get from Eq.(6) a one-dimensional diffusion equation

$$\dot{\rho}_t(X) = \frac{\partial}{\partial X} D(\rho_t(X)) \frac{\partial}{\partial X} \rho_t(X), \quad (8)$$

with a field-dependent diffusion coefficient

$$D(\rho_t(X)) = D_0 \left( 1 - 2\beta J \rho_t(X) (1 - \rho_t(X)) \right), \quad (9)$$

which is precisely the equation derived earlier by Lebowitz et al [19] and describing hydrodynamic limit dynamics of a system of mutual interacting particles undergoing ballistic motion. On the other hand, if we keep the second term on the rhs of Eq.(7), (which is appropriate if we consider some steady-state solutions [16]), we will obtain the customary equation of the form

$$\dot{\rho}_t(X) = \frac{\partial}{\partial X} M(\rho_t(X)) \frac{\partial}{\partial X} \frac{\delta \mathcal{F}(\rho_t(X))}{\delta \rho_t(X)}, \quad (10)$$

where the mobility  $M(\rho_t(X))$  is given by

$$M(\rho_t(X)) = \rho_t(X)(1 - \rho_t(X)), \quad (11)$$

while local free energy  $\mathcal{F}(\rho)$  obeys

$$\mathcal{F}(\rho) = \int dX \left( f(\rho) + \frac{\sigma^2 \beta J}{2} \left( \frac{\partial \rho}{\partial X} \right)^2 \right), \quad (12)$$

with

$$f(\rho) = \rho \ln \rho + (1 - \rho) \ln (1 - \rho) + \beta J \rho (1 - \rho). \quad (13)$$

Curiously enough,  $f(\rho)$ , which has been derived in our work starting from a microscopic dynamical model obeying the detailed balance condition, has exactly the same form as the phenomenological Flory-Huggins-de Gennes local free energy density [20, 21]. Note also that for  $\beta J \geq 2$ , the local free energy  $f(\rho)$  in Eq.(13) has a double-well structure whose minima approach 0 and 1 as  $\beta J$  increases. This implies that the Onsager mobility in Eq.(11) never reaches negative values, contrary to the behavior predicted by Eq.(8) for which one has  $D(\rho) < 0$  when  $\rho_{c,-} < \rho < \rho_{c,+}$ , with

$$\rho_{c,\pm} = \frac{1}{2} (1 \pm \sqrt{1 - 2/\beta J}). \quad (14)$$

Finally, we define the appropriate boundary conditions. As a matter of fact, any particle, in order to enter to the nanopore from the liquid phase, has to surmount an additional barrier  $E_M$  related to the enthalpic energy difference between the particle within the pore and in the bulk liquid phase [11, 12]. Supposing that the reservoir (bulk liquid phase) is in equilibrium with the particle phase within the single-file pore, we thus stipulate, following a similar analysis in [18], that the reservoir maintains a constant density  $\rho_F$  (see [11, 12] for relation between  $\rho_F$  and energetic parameters) at the entrance of the pore (site  $X = 0$  in Fig.2). Second boundary condition is rather evident, we just suppose that  $\rho_t(X)$  vanishes as  $X \rightarrow \infty$  at fixed  $t$ . Consequently, Eq.(6) (or Eq.(10)) is to be solved subject to the conditions

$$\rho_t(X = 0) = \rho_F, \quad \rho_t(X \rightarrow \infty) = 0. \quad (15)$$

Below we discuss solutions of Eqs.(6) and (10) obeying these two boundary conditions.

## Results

We focus here on the time-evolution of the total mass of particles  $M(t)$ , having entered the single-file pore up to time  $t$ , i.e.,

$$M(t) = \int_0^\infty dX \rho_t(X) \quad (16)$$

To define the time-dependence of  $M(t)$ , it is expedient to turn to the scaled variable  $\omega = X/2\sqrt{D_0 t}$ . In terms of this variable Eq.(10) attains the form

$$\begin{aligned} \frac{d^2 \rho(\omega)}{d\omega^2} + 2\omega \frac{d\rho(\omega)}{d\omega} - 2\beta J \frac{d}{d\omega} \left[ \rho(\omega) (1 - \rho(\omega)) \frac{d\rho(\omega)}{d\omega} \right] - \\ - \beta J \left( \frac{\sigma^2}{4D_0 t} \right) \frac{d}{d\omega} \left[ \rho(\omega) (1 - \rho(\omega)) \frac{d^3 \rho(\omega)}{d\omega^3} \right] = 0, \end{aligned} \quad (17)$$

while the boundary conditions in Eq.(15) become  $\rho(\omega = 0) = \rho_F$  and  $\rho(\omega \rightarrow \infty) = 0$ .

Note now that the term in the second line on the rhs of Eq.(17), associated with the second term in the expansion of the interaction energy in the Taylor series, Eq.(7), is irrelevant to the dynamics as  $t \rightarrow \infty$ , since it is multiplied by a vanishing function of time. Hence, the propagation dynamics can be adequately described by Eq.(8), which is not sufficient, however, for description of the steady-state characteristics, such as, e.g. steady-state particle current through a finite pore [16].

Now, in terms of the scaled variable  $\omega$ , the total mass of particles  $M(t)$  reads

$$M(t) = 2 m(J, \rho_F) \sqrt{D_0 t}, \quad (18)$$

where the prefactor  $m(J, \rho_F)$  is determined by

$$m(J, \rho_F) = \int_0^\infty d\omega \rho(\omega) \quad (19)$$

Consequently, Eq.(18), which can be thought of as the microscopic analog of the Washburn equation, signifies that the mass of particles grows in proportion to the square-root of time. Note that similar result has been obtained in [18] for  $J \equiv 0$ , in which case  $m(J, \rho_F) = \rho_F / \sqrt{\pi}$ .

Before we discuss behavior of the prefactor  $m(J, \rho_F)$ , it might be instructive to understand what are the physical processes underlying the  $M(t) \sim \sqrt{t}$  behavior (see also [18] for more detailed discussion). To do this, let us first recollect that the boundary condition  $\rho_t(X = 0) = \rho_F = \text{const}$  is tantamount to the assumption that the reservoir is in equilibrium with the particle phase in the pore. Turning next to the model depicted in Fig.2, we notice that a jump of the rightmost particle of the particle phase away of the reservoir, leads to creation of a "vacancy". When this vacancy manages to reach diffusively, due to redistribution of particles, the entrance of the pore, it perturbs the equilibrium and gets filled by a particle from the reservoir. Hence, the mass of particles within the pore  $M(t)$

is proportional to the current  $\mathcal{J}$  of vacancies from the front of the propagating phase<sup>1</sup>,  $M(t) \sim \mathcal{J}$ , where the current  $\mathcal{J} \sim 1/L$ ,  $L$  being the distance travelled by the rightmost particle away from the entrance of the pore. Consequently,  $M(t) \sim L \sim 1/L$ , which yields eventually the  $M(t) \sim \sqrt{t}$  law. Note also that, from the viewpoint of the underlying physics, the dynamical process under study is intrinsically related to such phenomena as directional solidification, freezing, limited by diffusive motion of the latent heat, or Stefan problem.

To define the prefactor  $m(J, \rho_F)$  we have solved Eq.(17) (with the last term set equal to zero) numerically, for various values of the system's parameters  $\rho_F$  and  $J$ . These results are summarized in Fig.3 where we depict  $m(J, \rho_F)$  as a function of  $\rho_F$  for several different values of  $\beta J$ .

Now, one notices that for any values of  $\rho_F$  and  $\beta J$  the prefactor  $m(J, \rho_F) > 0$ , which implies that, as one can expect on intuitive grounds, there is no transition in the one-dimensional system under study and the particle phase propagates into the pore as soon as  $\rho_F > 0$ . On the other hand, the prefactor  $m(J, \rho_F)$  depends on the system's parameters in a quite non-trivial fashion. While for relatively small  $\beta J$  the prefactor  $m(J, \rho_F)$  varies with  $\rho_F$  almost linearly, for large  $\beta J$  some saturation effect occurs, followed by, for larger  $\beta J$ , a non-monotoneous  $\rho_F$ -dependence, and eventually, after a cusp-like variation, with a rapid growth.

We begin with a small  $\beta J$  limit, in which case some perturbative analytical calculations are possible. To do this, let us represent  $\rho(\omega)$  in the form of the series

$$\rho(\omega) = \sum_{n=0}^{\infty} (2\beta J)^n \rho_n(\omega), \quad (20)$$

(which is related to expansion in powers of the reservoir density  $\rho_F < 1$ , as we will see in what follows) and try to calculate explicitly several first terms in such an expansion, constraining ourselves to the quadratic in  $\beta J$  approximation. After some rather cumbersome but straightforward calculations, we find eventually, that in the quadratic with respect to the parameter  $2\beta J$  approximation, the prefactor  $m(J, \rho_F)$  obeys:

$$\begin{aligned} m(J, \rho_F) &= \frac{\rho_F}{\sqrt{\pi}} - (2\beta J) \left[ 0.18 \rho_F^2 - 0.134 \rho_F^3 \right] \\ &- (2\beta J)^2 \left[ 0.025 \rho_F^3 - 0.047 \rho_F^4 + 0.018 \rho_F^5 \right] \end{aligned} \quad (21)$$

---

<sup>1</sup>Note, however, that there are some subtleties concerning propagation of the rightmost particle of the phase growing in the single-file pore. As a matter of fact, it has been shown in [18] that in a similar model without attractive interactions (i.e.  $J = 0$ ) the mean displacement of the rightmost particle follows  $\bar{X}(t) \sim \sqrt{t \ln(t)}$ , i.e. grows at a faster rate than the mass  $M(t)$ . Similar behavior is observed for the front of the phase, propagating in the single-file pore, also in the interacting case, i.e. for arbitrary  $J$  [16].

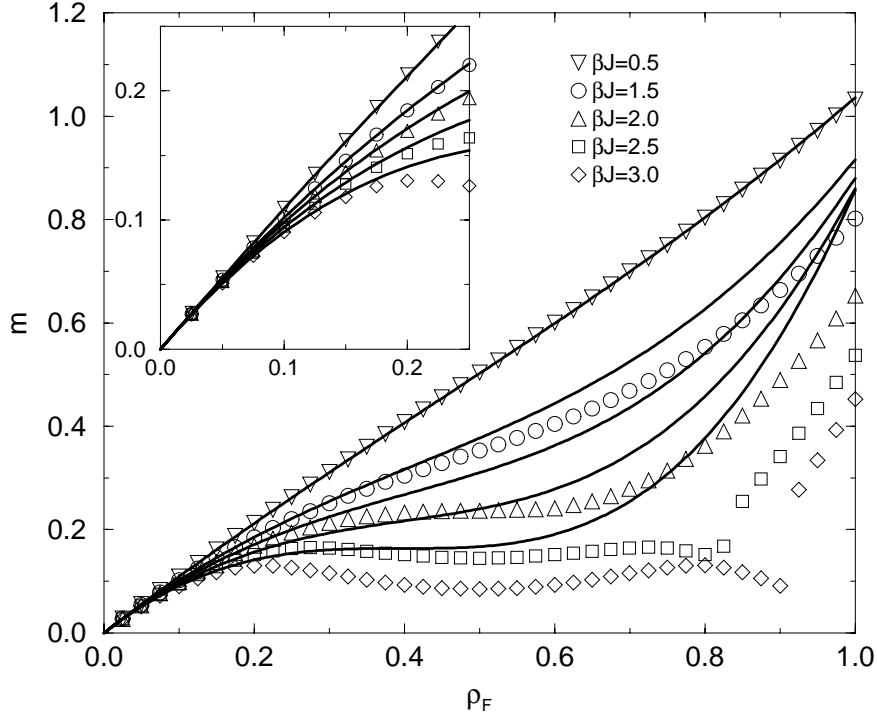


Figure 3: The prefactor  $m = m(J, \rho_F)$  versus the density  $\rho_F$  for different values of the amplitude  $J$  of the attractive particle-particle interactions. Symbols denote the results of numerical solution of Eq.(17), while the solid lines correspond to the analytical result in Eq.(21). The inset displays the behavior for small  $\rho_F$ .

This dependence, as one notices, agrees quite well with the numerical solution for relatively low values of  $\beta J$  over the entire domain of variation of  $\rho_F$ , or, for larger  $\beta J$ , for progressively smaller values of  $\rho_F$ .

To get some understanding of the intricate, non-trivial behavior of  $m(J, \rho_F)$ , observed for larger values of  $\beta J$ , we analyse dynamical density profiles defined by Eq.(8) versus  $X$  and  $X/M(t)$  for  $\beta J = 3$  and different reservoir densities  $\rho_F$ , (see Fig.4). Note now that the form of the density profiles is rather complex and depends largely on whether  $\rho_F$  is less than or exceeds  $\rho_{c,\pm}$ . When  $\rho_F \leq \rho_{c,-}$ , the form of the density profile is well described by  $\rho_t(X) = \rho_F \text{erfc}(X/M(t))$ , where  $\text{erfc}(X/M(t))$  is the error function. This behavior is essentially the same as the one predicted for non-interacting lattice gas in [18]. On the other hand, when  $\rho_F$  exceeds  $\rho_{c,-}$ , but is less than  $\rho_{c,+}$  (for  $\beta J = 3$ ,  $\rho_{c,\pm}$  are equal to 0.79 and 0.21, respectively) we have two different regimes: the density rapidly, within the small constant distance  $l(\rho_F)$ , drops to the value  $\rho_{c,-}$  and then evolves as  $\rho_t(X) = \rho_{c,-} \text{erfc}(X/M(t))$ , where

$\rho_{c,-}$  is independent of  $\rho_F$ . Since, the prefactor  $m(J, \rho_F)$  is just an integral of  $\rho_t(X)$ , we have, hence, two contributions: the first is the integral over the interval  $[0, l(\rho_F)]$ , which is weakly dependent on  $\rho_F$  and the second one - the integral over  $[l(\rho_F), \infty[$ , which is independent of  $\rho_F$  and gives the bulk contribution to  $m(J, \rho_F)$ . These two contributions define the plateau-like part in the dependence of  $m(J, \rho_F)$  on  $\rho_F$ . On the other hand, when  $\rho_F$  exceeds  $\rho_{c,+}$  and hence  $D(\rho)$  is positive definite, a dense droplet-like structure emerges near the entrance of the pore, which grows in size in proportion to  $\sqrt{t}$  and contains most of the particles. This phenomenon explains apparently the growth of  $m(J, \rho_F)$  with  $\rho_F$  observed for  $\rho_F \geq \rho_{c,+}$ .

## Conclusions

In conclusion, we have studied propagation dynamics of a particle phase emerging in a single-file pore connected to a reservoir of particles (bulk liquid phase). Modelling the pore as a semi-infinite one-dimensional regular lattice, whose sites support, at most, a single occupancy, and supposing that the particles interaction potential consists of an abrupt, hard-core repulsive part, and is attractive, with an amplitude  $J \geq 0$ , for the nearest-neighboring particles, we derived the dynamical equation describing the time-evolution for the local particle density. This equation has been analysed both analytically and numerically. Within our approach, we defined the evolution of the total number  $M(t)$  of particles entering the single-file pore up to time  $t$  and also discussed the dynamics of the density distribution function within the pore. We have shown that the growth of  $M(t)$  is described by  $M(t) = 2m(J, \rho_F)\sqrt{D_0 t}$ , which can be thought of as the microscopic analog of the Washburn equation, where  $D_0$  denotes the "bare" diffusion coefficient, while the prefactor  $m(J, \rho_F)$  is a non-trivial function of the attractive interactions amplitude  $J$  and the density  $\rho_F$  at the entrance to the pore. We have discussed a peculiar behavior of  $m(J, \rho_F)$  and explained it through the analysis of the dynamical density distribution within the pore.

## References

- [1] *Access in Nanoporous Materials*, eds. T.J.Pinnavaia and M.F.Thorpe (Plenum, New York, 1995)
- [2] M.Sahimi, *Flow and Transport in Porous Media and Fractured Rock*, (VCH, Weinheim, Germany, 1995)

- [3] N.Y.Chen, J.T.F.Degnan and C.M.Smith, *Molecular Transport and Reaction in Zeolites*, (VCH, New York, 1994)
- [4] B.Alberts, D.Bray and J.Lewis, *Molecular Biology of the Cell*, (Garland, New York, 1994)
- [5] W.M.Meier and D.H.Olson, *Atlas of Zeolite Structure Types*, (Butterworths, London, 1987)
- [6] V.Gupta et al., Chem. Phys. Lett. **247**, 596 (1995)
- [7] V.Kukla et al., Science **272**, 702 (1996)
- [8] D.Keffer, A.V.McCormick and H.T.Davis, Mol. Phys. **87**, 367 (1996)
- [9] K.Hahn, J.Kärger and V.Kukla, Phys. Rev. Lett. **76**, 2762 (1996)
- [10] C.Rödenbeck, J.Kärger and K.Hahn, Phys. Rev. E **55**, 5697 (1997)
- [11] T.Chou, Phys. Rev. Lett. **80**, 85 (1998)
- [12] T.Chou, J. Chem. Phys. **110**, 606 (1999)
- [13] S.Murad, P.Ravi and J.G.Powles, J. Chem. Phys. **98**, 9771 (1993)
- [14] D.S.Sholl and K.A.Fichthorn, J. Chem. Phys. **107**, 4384 (1997)
- [15] L.Xu et al., Phys. Rev. Lett. **80**, 3511 (1998)
- [16] A.M.Lacasta, J.M.Sancho, F.Sagues and G.Oshanin, in preparation
- [17] G.Giacomin and J.L.Lebowitz, Phys. Rev. Lett. **76**, 1094 (1996)
- [18] S.F.Burlatsky, G.Oshanin, A.M.Cazabat and M.Moreau, Phys. Rev. Lett. **76**, 86 (1996)
- [19] J.Lebowitz, E.Orlandi and E.Presutti, J. Stat. Phys. **63**, 933 (1991)
- [20] P.G.de Gennes, J. Chem. Phys. **72**, 4756 (1980)
- [21] K.Binder, J. Chem. Phys. **79**, 6387 (1983)

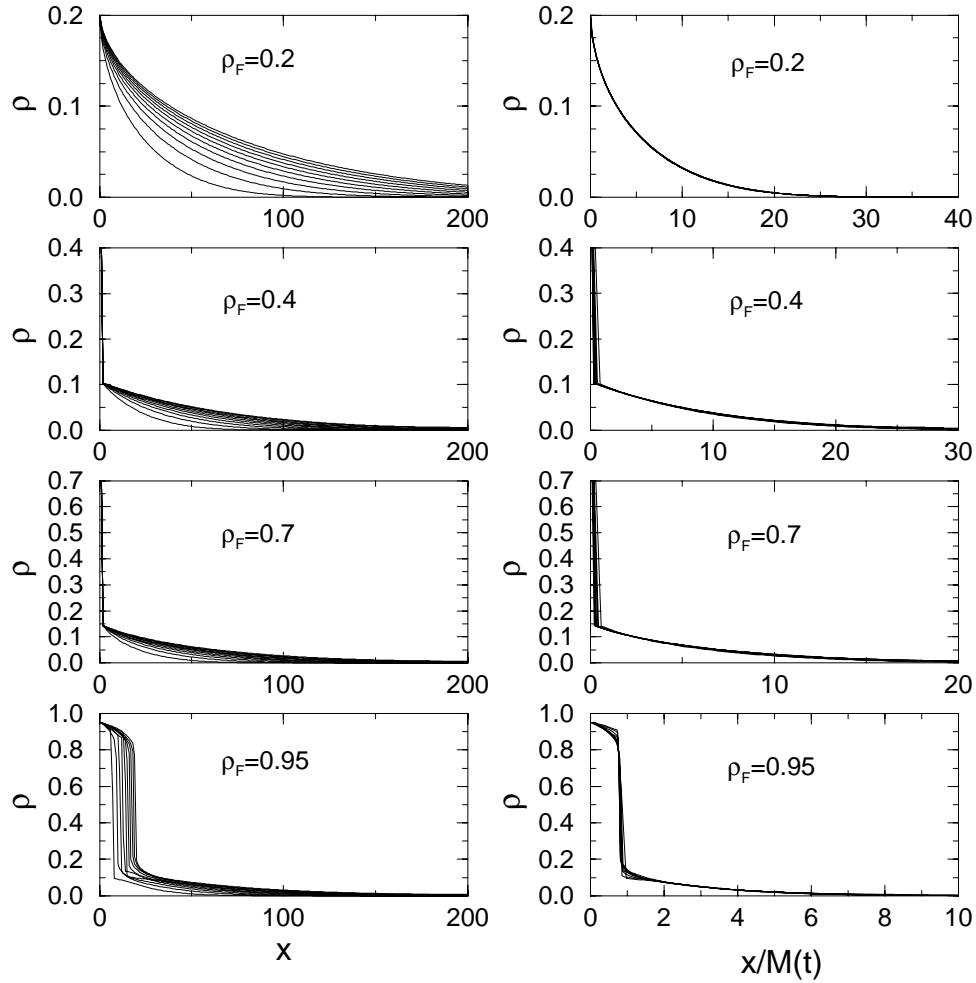


Figure 4: Dynamical density profiles defined by Eq.(8) for  $\beta J = 3$  and different values of  $\rho_F$ . In the left column  $\rho_t(X)$  is plotted versus the space variable  $X$  and here different curves on each graph show the dynamics of the density distribution in the single-file pore, Eq.(6), while in the right column we present corresponding plots for  $\rho_t(X)$  vs the scaling variable  $X/M(t)$ .